Supplementary information for "Photonic heat transport through a Josephson junction in a resistive environment"

A. Levy Yeyati,[1] D. Subero,[2] J. P. Pekola,[2] and R. Sánchez[1]

[1]*Departamento de Física Teórica de la Materia Condensada, Condensed Matter Physics Center (IFIMAC), and Instituto Nicolás Cabrera, Universidad Autónoma de Madrid, 28049 Madrid, Spain*

[2]*PICO Group, QTF Centre of Excellence, Department of Applied Physics, Aalto University School of Science, P.O. Box 13500, 0076 Aalto, Finland*

S-I. DETAILS ON NUMERICAL CALCULATIONS

A. Self-energies

From Eq. (8) in the main text, the zero order GFs in time representation are given by

$$D_0^r(t) = -\frac{\theta(t)}{m\omega_1} e^{-\gamma t/2} \sinh(\omega_1 t)$$
$$D_0^K(t) = S_1(t) + S_2(t) \tag{S1}$$

where $\gamma = (\eta_L + \eta_R)/m$, $\omega_1 = \sqrt{\gamma^2/4 - \omega_c^2}$ and

$$S_1(t) = -\sum_{\mu=L,R} \frac{\eta_\mu}{2m\omega_1\gamma}\left(\coth\left(\frac{\beta_\mu\lambda_1}{2}\right)e^{i\lambda_1|t|} - \coth\left(\frac{\beta_\mu\lambda_2}{2}\right)e^{i\lambda_2|t|}\right)$$

$$S_2(t) = 4i\sum_{\mu=L,R}\frac{\eta_\mu}{m\beta_\mu}\sum_{n>0}\frac{\nu_n^\mu e^{-\nu_n^\mu|t|}}{\left(\omega_c^2 + (\nu_n^\mu)^2\right)^2 - \gamma^2(\nu_n^\mu)^2}\,, \tag{S2}$$

where $\lambda_{1,2} = i(\gamma/2 \pm \omega_1)$, and $\nu_n^\nu = 2n/\beta_\nu$ are the Matsubara frequencies.

By introducing these analytical expressions for the propagators in time representation into Eqs. (12) in the main text and performing their Fourier transform numerically, we obtain the results shown in Fig. 2 for the different self-energies in frequency space. For comparison we show the corresponding results for the series configuration.

In Fig. S2 we show the inelastic contribution to the heat current in the series configurations for the same parameters as in Fig. 3(a) in the main text. As can be observed, this contribution is positive so that it tends to increase the total heat current when added to the elastic contribution.

S-II. ANALYTICAL APPROXIMATIONS

Here we give details on the approximations used to obtain the analytic behaviour of the self-energies $\Sigma^{r(2)}(\omega)$ and $\Sigma^{K(2)}(\omega)$ in the parallel configuration.

A. Retarded self-energy

We start with the time-dependent retarded selfenergy as expressed in Eq. (12) in the main text:

$$\Sigma^{r(2)}(t) = E_J^2 \sin\frac{D_0^r(t)}{2}\exp\left[\frac{i}{2}\left(D_0^K(t) - D_0^K(0)\right)\right] - B\delta(t), \tag{S3}$$

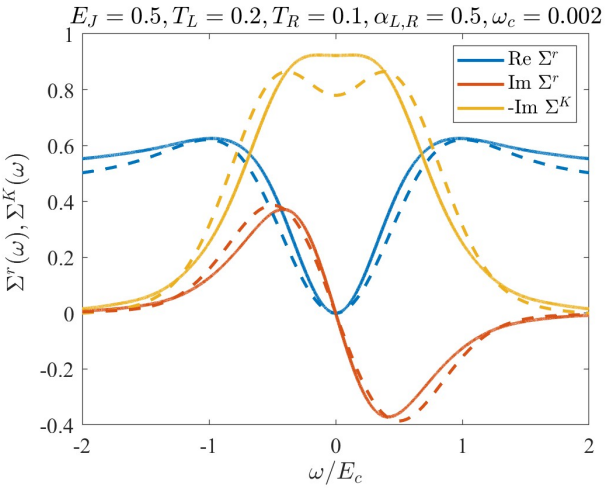

FIG. S1. Self-energies in frequency representation obtained numerically from Eqs. (12) in the main text. Energies in units of E_c. The corresponding parameters are indicated in the figure title. The dashed lines correspond to the self-energies in the series configuration for the same set of parameters.

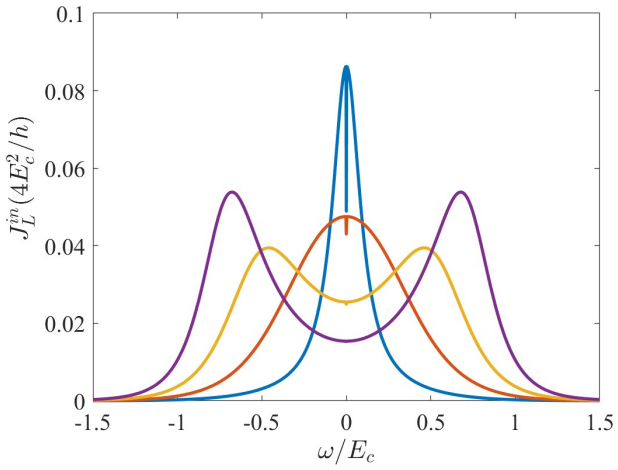

FIG. S2. Inelastic contribution to the heat current in the series configuration for the same parameters as in Fig. 3(a) in the main text.

of which we want to obtain the Fourier transform. For this, we consider the first term:

$$\tilde{\Sigma}(t) = E_J^2 \sin\frac{D_0^r(t)}{2}\exp\left[\frac{i}{2}\left(D_0^K(t) - D_0^K(0)\right)\right]. \tag{S4}$$

The second term, proportional to B will be cancelled out with $\tilde{\Sigma}(0)$. We can simplify it by writing $D_0^r(t) = D_0^a(-t) = -\theta(t)(1-\exp[-\gamma t])/m\gamma$, and using the approximation

$$\mathrm{Re}\left[\frac{i}{2}(D_0^K(t)-D_0^K(0))\right] \approx -\sum_\mu \frac{\eta_\mu}{\pi m^2\gamma^2}\ln\left[\frac{\gamma\beta_\mu}{\pi}\sinh\left(\frac{\pi|t|}{\beta_\mu}\right)\right] \tag{S5}$$

for $|\gamma t| \gg 1$ and $k_B T \ll \gamma$ [S1]. Doing so, we get:

$$\tilde{\Sigma}(t) = \theta(t)E_J^2 \sin\left(\frac{e^{-\gamma t}-1}{2m\gamma}\right)\prod_\mu\left[\frac{\gamma\beta_\mu}{\pi}\sinh\left(\frac{\pi|t|}{\beta_\mu}\right)\right]^{-\eta_\mu/\pi m^2\gamma^2}, \tag{S6}$$

where $\eta_\mu = R_Q/2\pi R_\mu$, $m = \hbar/E_C$ and $\gamma = \sum_\mu \eta_\mu/m$, as defined in the main text. We need to solve its Fourier transform:

$$\tilde{\Sigma}(\omega) = \mathcal{A}\gamma\int_0^\infty dt \sin\left(\frac{e^{-\gamma t}-1}{2m\gamma}\right)\prod_\mu\left[2\sinh\left(\frac{\pi|t|}{\beta_\mu}\right)\right]^{-\frac{\eta_\mu}{\pi m^2\gamma^2}} e^{i\omega t}, \tag{S7}$$

where we have defined the prefactor

$$\mathcal{A} \equiv \frac{E_J^2}{\gamma}\prod_\mu\left(\frac{\gamma\beta_\mu}{2\pi}\right)^{-\eta_\mu/\pi m^2\gamma^2}. \tag{S8}$$

To reach the low frequency limit $T_j \gg \omega$, we approximate $\sinh(\pi|t|/\beta_\mu) \approx e^{\pi|t|/\beta_\mu}/2$. Then, performing the change of variables $u = e^{-\gamma t}$ we get:

$$\tilde{\Sigma}(\omega) = \mathcal{A}\int_0^1 du \sin\left(\frac{u-1}{2m\gamma}\right)u^{c-1}, \tag{S9}$$

with

$$c \equiv \frac{1}{m^2\gamma^3}\left(\frac{\eta_L}{\beta_L}+\frac{\eta_R}{\beta_R}\right) - \frac{i\omega}{\gamma}. \tag{S10}$$

The integral in Eq. (S9) has an analytical solution if $\mathrm{Re}(c) > 0$:

$$\int_0^1 du \sin[a(u-1)]u^{c-1} = g_1(a,c) + g_2(a,c), \tag{S11}$$

with

$$\begin{aligned} g_1(a,c) &= \frac{\cos(a)}{(1+c)/a}\,{}_1F_2\left(\frac{1+c}{2};\frac{3}{2},\frac{3+c}{2};-\frac{a^2}{4}\right) \\ g_2(a,c) &= -\frac{\sin(a)}{c}\,{}_1F_2\left(\frac{c}{2};\frac{1}{2},\frac{2+c}{2};-\frac{a^2}{4}\right), \end{aligned} \tag{S12}$$

and where ${}_1F_2(a_1;b_1,b_2;z)$ is a "generalized hypergeometric function". Formally, this then gives an analytical solution:

$$\tilde{\Sigma}(\omega) = \mathcal{A}\left[g_1\left(\frac{1}{2m\gamma},c\right)+g_2\left(\frac{1}{2m\gamma},c\right)\right], \tag{S13}$$

but it is not very informative until we plot its real and imaginary parts, which is done in Fig. S3.

In a linear expansion, the constant term is real, giving the value of B in Eq. (S3), and the linear term is pure imaginary, so the linear expansion simplifies to:

$$\tilde{\Sigma}(\omega) = i\mathcal{A}\mathrm{Im}\left[(g_1'+g_2')\big|_{\omega=0}\right]\omega. \tag{S14}$$

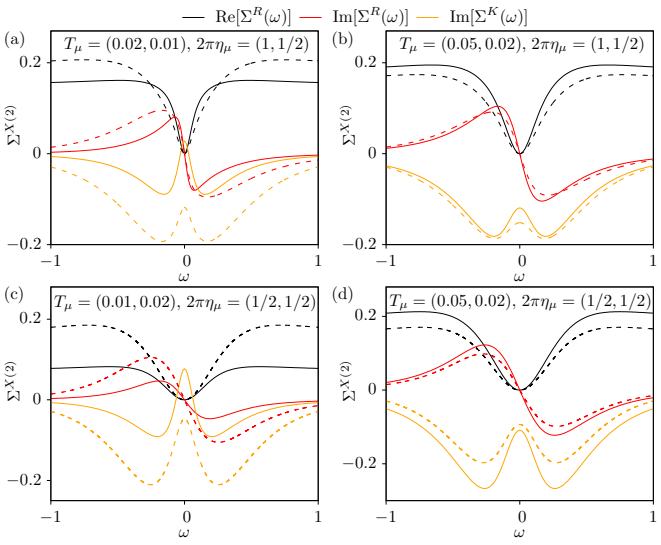

FIG. S3. Self-energies for different temperatures $T_\mu = (T_L, T_R)$ and damping parameters $\eta_\mu = (\eta_L, \eta_R)$. (a) and (b): asymmetric case with $\eta_L = 1/2\pi$ and $\eta_R = 1/4\pi$. (c) and (d): symmetric case with $\eta_L = \eta_R = 1/4\pi$. Dashed lines show the numerical results. In all panels, $E_J = 0.2$, $m = 1$.

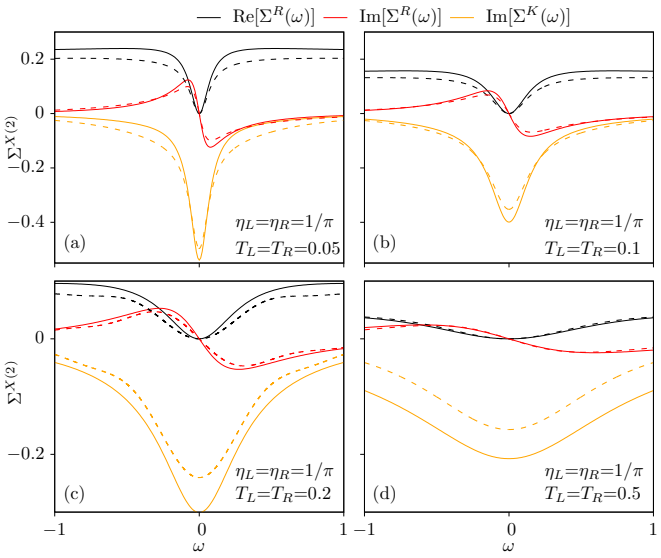

FIG. S4. Comparison of numeric and analytic selfenergies in the low impedance regime, $R_\mu = 0.5R_Q$, for increasing temperatures. Other parameters are as in Fig. S3.

B. Keldysh self-energy

Now we consider the time-dependent Keldysh self-energy in Eq. (12) in the main text:

$$\Sigma^{K(2)}(t) = \frac{E_J^2}{i}\cos\left(\frac{D_0^r(t)}{2}\right)\cos\left(\frac{D_0^a(t)}{2}\right)\exp\left[\frac{i}{2}\left(D_0^K(t)-D_0^K(0)\right)\right]. \tag{S15}$$

We separate the time integral in the Fourier transform in two terms, with $D_0^r(t<0)=0$ and $D_0^a(t>0)=0$:

$$\Sigma^{K(2)}(\omega) = -i\mathcal{A}\gamma\left\{\int_{-\infty}^{0} dt\cos\left(\frac{e^{\gamma t}-1}{2m\gamma}\right)\prod_\mu\left[2\sinh\left(\frac{-\pi t}{\beta_\mu}\right)\right]^{\frac{-\eta_\mu}{\pi m^2\gamma^2}} e^{i\omega t} + \int_0^{\infty} dt\cos\left(\frac{e^{-\gamma t}-1}{2m\gamma}\right)\prod_\mu\left[2\sinh\left(\frac{\pi t}{\beta_\mu}\right)\right]^{\frac{-\eta_\mu}{\pi m^2\gamma^2}} e^{i\omega t}\right\}, \tag{S16}$$

where we have again used the approximation in Eq. (S5) [S1]. Doing a change $t\to -t$ in the first integral of Eq. (S16), we can write

$$\Sigma^{K(2)}(t) = -i\mathcal{A}\gamma\left(\mathcal{I}^+ + \mathcal{I}^-\right), \tag{S17}$$

with

$$\mathcal{I}^{\pm} = \int_0^{\infty} dt\cos\left(\frac{e^{-\gamma t}-1}{2m\gamma}\right)\prod_\mu\left[2\sinh\left(\frac{\pi t}{\beta_\mu}\right)\right]^{\frac{-\eta_\mu}{\pi m^2\gamma^2}} e^{\pm i\omega t}. \tag{S18}$$

Following the same steps as for the retarded case ($u=e^{-\gamma t}$), we arrive to:

$$\Sigma^{K(2)} = -i\mathcal{A}\int_0^1 du\cos\left(\frac{u-1}{2m\gamma}\right)\left(u^{c-1}+u^{c^*-1}\right) \tag{S19}$$

In this case, we can use the integral:

$$\int_0^1 du\cos[a(u-1)]u^{c-1} = g_3(a,c)+g_4(a,c), \tag{S20}$$

with

$$\begin{aligned} g_3(a,c) &= \frac{\cos(a)}{c}\,{}_1F_2\left(\frac{c}{2};\frac{1}{2},\frac{2+c}{2};-\frac{a^2}{4}\right)\\ g_4(a,c) &= a\frac{\sin(a)}{1+c}\,{}_1F_2\left(\frac{1+c}{2};\frac{3}{2},\frac{3+c}{2};-\frac{a^2}{4}\right), \end{aligned} \tag{S21}$$

provided $\mathrm{Re}(c)>0$. We note that $g_3(1/2m\gamma,c^*)=g_3^*(1/2m\gamma,c)$ and $g_4(1/2m\gamma,c^*)=g_4^*(1/2m\gamma,c)$. Hence, the Keldysh self-energy is purely imaginary:

$$\Sigma^{K(2)} = -i2\mathcal{A}\mathrm{Re}\left[g_3\left(\frac{1}{2m\gamma},c\right)+g_4\left(\frac{1}{2m\gamma},c\right)\right]. \tag{S22}$$

The result is plotted in orange lines in Fig. S3.

C. Frequency expansion

We can expand on the integrand of Eqs. (S9) and (S19) for low frequencies, getting:

$$\Sigma^{\alpha(2)} \approx \Sigma_0^{\alpha(2)} + \omega\Sigma_1^{\alpha(2)} + \omega^2\Sigma_2^{\alpha(2)}, \tag{S23}$$

with

$$\Sigma_k^{r(2)} = -\frac{1}{k!}\left(\frac{i}{\gamma}\right)^k \mathcal{A}\mathcal{I}_k(c_0) \tag{S24}$$

$$\Sigma_0^{K(2)} = -2i\mathcal{A}\int_0^1 du\cos\left(\frac{u-1}{2m\gamma}\right)u^{c_0-1} \tag{S25}$$

$$\Sigma_1^{K(2)} = 0 \tag{S26}$$

$$\Sigma_2^{K(2)} = \frac{i}{\gamma^2}\mathcal{A}\int_0^1 du\cos\left(\frac{u-1}{2m\gamma}\right)u^{c_0-1}\ln^2 u, \tag{S27}$$

where

$$c_0 \equiv c(\omega=0) = \frac{1}{m^2\gamma^3}\left(\frac{\eta_L}{\beta_L}+\frac{\eta_R}{\beta_R}\right) \tag{S28}$$

and

$$\mathcal{I}_k(c_0) = \int_0^1 du\sin\left(\frac{u-1}{2m\gamma}\right)u^{c_0-1}\ln^k u. \tag{S29}$$

These integrals again have analytical solutions in terms of hypergeometric functions of higher order. For this, we define:

$$\mathcal{G}^{(n)}_{pqs} = {}_nF_{n+1}\left(\frac{p+c_0}{2}1_n;\frac{q}{2},\frac{s+c_0}{2}1_n;-\frac{1}{16m^2\gamma^2}\right), \tag{S30}$$

where 1_n is a list of n units.With these, we write:

$$\begin{aligned} \mathcal{I}_0(c_0) &= \frac{\cos\left(\frac{1}{2m\gamma}\right)}{2m\gamma(1+c_0)}\mathcal{G}^{(1)}_{1,3,3} - \frac{\sin\left(\frac{1}{2m\gamma}\right)}{c_0}\mathcal{G}^{(1)}_{0,1,2}\\ \mathcal{I}_1(c_0) &= -\frac{2m\gamma(1+2c_0)\cos\left(\frac{1}{2m\gamma}\right)\sin\left(\frac{1}{2m\gamma}\right)}{c_0^2(1+c_0)^2}\\ &\quad+\frac{\cos\left(\frac{1}{2m\gamma}\right)}{12m^2\gamma^2(1+c_0)(3+c_0)}\left[\frac{\mathcal{G}^{(1)}_{3,5,5}}{1+c_0}+\frac{\mathcal{G}^{(2)}_{3,5,5}}{3+c_0}\right]\\ &\quad-\frac{\sin\left(\frac{1}{2m\gamma}\right)}{2m\gamma c_0^2(2+c_0)^2}\left[(2+c_0)\mathcal{G}^{(1)}_{2,3,4}+c_0\mathcal{G}^{(2)}_{2,3,4}\right]\\ \mathcal{I}_2(c_0) &= 2\left[\frac{\cos\left(\frac{1}{2m\gamma}\right)}{2m\gamma(1+c_0)^3}\mathcal{G}^{(3)}_{2,3,3}-\frac{\sin\left(\frac{1}{2m\gamma}\right)}{c_0^3}\mathcal{G}^{(3)}_{0,1,2}\right]. \end{aligned} \tag{S31}$$

For the Keldysh self-energy, it is sufficient to look at the value at the origin, $\Sigma^{K(2)}(\omega)=\Sigma_0^{K(2)}+O(\omega^2)$:

$$\Sigma_0^{K(2)} = -2i\mathcal{A}\left[\frac{\cos\left(\frac{1}{2m\gamma}\right)}{c_0}\mathcal{G}^{(1)}_{0,1,2}+\frac{\sin\left(\frac{1}{2m\gamma}\right)}{2m\gamma(1+c_0)}\mathcal{G}^{(1)}_{1,3,3}\right]. \tag{S32}$$

1. *Low temperature scaling*

The linear coefficient of the retarded self-energy corresponds to the damping parameter correction, $\delta\eta$, defined in the main text. Taking the low temperature limit in the above expressions it is straightforward to show that for $T_{L,R}\ll\gamma$ and $m\gamma\sim 1/(2\pi)$

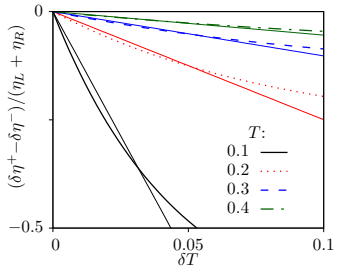

FIG. S5. Rectification effect as a function of the temperature difference using the approximation of Eq. (S36), for different temperatures. Thin solid lines correspond to the linear expansion of Eq. (S38). Parameters: $E_J = 0.2$, $m = 1$, $\eta_L = 1/\pi$, $\eta_R = 1/4\pi$.

$$\delta\eta \sim \mathcal{A}\frac{\gamma}{c_0^2} \equiv \left(\frac{E_J}{\gamma}\right)^2 \frac{\left(\frac{T_L}{\gamma}\right)^{\frac{\eta_L}{\pi m^2\gamma^2}}\left(\frac{T_R}{\gamma}\right)^{\frac{\eta_R}{\pi m^2\gamma^2}}}{\left(\frac{\eta_L T_L + \eta_R T_R}{m^2\gamma^2}\right)^2} \,. \tag{S33}$$

In the limit $T_L = T_R = T$ the scaling reduces to $\delta\eta \sim T^{2/\alpha-2}$, where $\alpha = 2\pi(\eta_L + \eta_R)$ is the inverse of the total resistance in units of R_Q, which signals the SB transition at $\alpha = 1$ [S1].

Based on this scaling it is possible to determine the transition point T^* for heat transport indicated in Figs. 2(c) and 3(c) of the main text. For that purpose remind that at low frequency the heat transmission coefficient scales as $\eta/\bar{\eta}$ for a symmetric case with $\eta_L = \eta_R = \eta$ (see Eq. (14) in main text). Thus, in order to get the same heat current for two cases with different resistances at the same mean temperature we need

$$\frac{\bar{\eta}_1}{\eta_1} = \frac{\bar{\eta}_2}{\eta_2} \longrightarrow \frac{T^{2/\alpha_1-2}}{\gamma_1^{2/\alpha_1+1}} = \frac{T^{2/\alpha_2-2}}{\gamma_2^{2/\alpha_2+1}} \,. \tag{S34}$$

Setting $\alpha_1 = 1$ in the limit $\alpha_2 \to 1$ we obtain $T = T^* = 1/(2\pi e^{3/2}) \simeq 0.036$, in agreement with the numerical results in Figs. 2(c) and 3(c) of the main text.

S-III. RECTIFICATION

The term $\Sigma_1^{r(2)}$ modifies the damping parameter $\Sigma_1^{r(2)} = -i\delta\eta$, which affects the transmission probability. If the resistances are different, the response is different depending on their temperature. Linearizing Eq. (14) in the main text at $\omega = 0$:

$$\tau_{\rm eff}^{\pm} \approx \frac{4\eta_L\eta_R}{(\eta_L+\eta_R)^2}\left(1 - \frac{\delta\eta^{\pm}}{\eta_L+\eta_R}\right). \tag{S35}$$

A rectification effect appears when $\delta\tau^{\rm eff}_{\rm parallel} = \tau^+_{\rm eff} - \tau^-_{\rm eff} \neq 0$:

$$\delta\tau^{\rm eff}_{\rm parallel} \approx \frac{4\eta_L\eta_R}{(\eta_L+\eta_R)^3}\left(\delta\eta^- - \delta\eta^+\right). \tag{S36}$$

We hence need

$$\delta\eta^- - \delta\eta^+ = i\left[\Sigma^{r(2)}_{1,L} - \Sigma^{r(2)}_{1,R}\right] \tag{S37}$$

to be finite, where $\Sigma^{r(2)}_{1,\mu}$ is defined as the linear coefficient $\Sigma^{r(2)}_1$ when terminal μ is at temperature $T + \delta T$ and the other one is at T. They are obtained using Eqs. (S24) and (S31). The result is plotted in Fig. S5 as a function of the temperature difference δT.

We gain further insight by assuming a small temperature difference δT, so we can linearize use the scaling of Eq. (S33), getting

$$\delta\eta^- - \delta\eta^+ \approx (mE_J)^2\frac{\eta_R-\eta_L}{\eta_L+\eta_R}\left(\frac{2}{\alpha}-2\right)T^{\frac{2}{\alpha}-2}\frac{\delta T}{T}, \tag{S38}$$

see Fig. S5. This expression gives the scaling of the rectification coefficient:

$$\mathcal{R} - 1 \sim (mE_J)^2\frac{\eta_R-\eta_L}{\eta_L+\eta_R}\left(\frac{2}{\alpha}-2\right)T^{\frac{2}{\alpha}-2}\frac{\delta T}{T} \tag{S39}$$

given in the main text.

A. Current-voltage characteristics

In the case of the current-voltage characteristics, the perturbative analysis carried out in this work leads to the well known result [S2]

$$I(V) = \frac{\pi e E_J^2}{\hbar}\left[P(2eV) - P(-2EV)\right] \,, \tag{S40}$$

with the function

$$P(\omega) = \frac{1}{2\pi\hbar}\int_{-\infty}^{\infty} dt \exp\left[\mathcal{J}(t) + i\omega t\right] \,,$$

and where

$$\mathcal{J}(t) = 2\int_{-\infty}^{\infty}\frac{d\omega}{\omega}\frac{{\rm Re}[Z_t(\omega)]}{R_Q}\frac{e^{-i\omega t}-1}{1-e^{-\beta\omega}}$$

is the phase correlation function, with $Z_t(\omega) = Z_L(\omega) + Z_R(\omega)$. This expression was used to fit the current-voltage characteristic in Ref. [S3].

B. Evidence of insulating behavior in the data of Ref. [S3]

According to Fig. 3(c) in the main text, a junction in the insulating side of the SB transition should exhibit decreasing heat conductance for $\bar{T} \to 0$, while it should saturate to a finite value on the superconducting side. The data shown in Fig. S6, taken from Ref. [S3], would be thus compatible insulating behavior. A detailed comparison with theory would require, however, measurements in a extended temperature range.

[S1] U. Eckern and F. Pelzer, Quantum Dynamics of a Dissipative Object in a Periodic Potential, Europhys. Lett. **3**, 131 (1987).

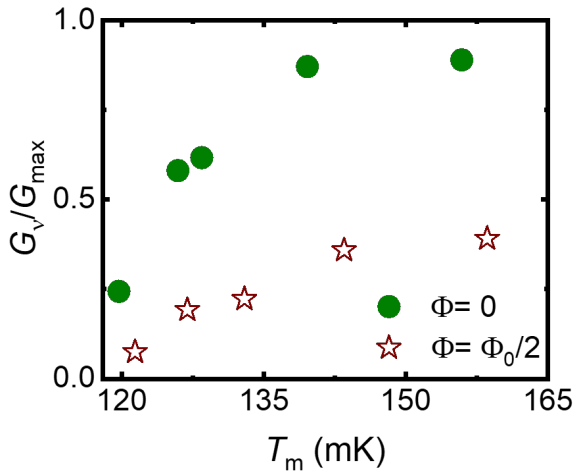

FIG. S6. Thermal conductance obtained from the data in Ref. [S3] normalized to the maximum thermal conductance for a quantum channel. The full dots correspond to zero flux (maximum E_J) while the open symbols corresponds to half flux quantum through the SQUID where $E_J \to 0$.

[S2] G.-L. Ingold and Y. V. Nazarov, Charge tunneling rates in ultrasmall junctions, in Single Charge Tunneling, edited by H. Grabert and M. Devoret (Springer, 1992) Chap. 2, p. 21.

[S3] D. Subero, O. Maillet, D. S. Golubev, G. Thomas, J. T. Peltonen, B. Karimi, M. Marín-Suárez, A. L. Yeyati, R. Sánchez, S. Park, and J. P. Pekola, Bolometric detection of coherent Josephson coupling in a highly dissipative environment, Nature Comm. **14**, 7924 (2023).